CRACK INITIATION AND CRACK GROWTH IN PM ASTROLOY UNDER HTLCF CONDITIONS

J. BRESSERS*

Selected data on the crack initiation and on the growth of cracks under high temperature low cycle fatigue conditions are presented for PM Astroloy, a disk material for application in aero gas turbines. The crack initiation life and the life to failure are strongly influenced by several time dependent processes (oxidation, time dependent deformation, dynamic strain ageing), operating individually or simultaneously depending on the testing conditions. The crack growth data show a "short" crack behaviour up to crack sizes of the order of ten times the grain size, their growth rates largely exceeding those of "long" cracks. In view of the life time criterion adopted in the design of aero gas turbine disks, "long" crack growth data are, therefore, unconservative.

INTRODUCTION

In normal practice two types of fatigue data are currently obtained and used in engineering design and in performance assessment: endurance data and long crack growth data. The former, integrated type of data does not distinguish between the respective contributions of crack initiation and of crack growth to the total fatigue life. Long crack growth data, described in terms of fracture mechanics parameters, yield a differential type of information on only one stage of the fatigue life. Data relating to the growth of microcracks are virtually non-existent. In particular applications, such as for example in aero gas turbine disks, the life fractions spent in the initiation and in the growth of microcracks make up an important fraction of their total life. Crack growth characteristics of disk materials are becoming an essential element in the design of disks in view of the trend to the retirement of disks for cause and the concomitant adoption of "defect tolerant" design approaches. The maximum crack size of approximately 0.8 mm which is tolerated in disks calls for a comparison between long and short crack data under conditions typical for the disk operating regime. Short cracks have been shown to grow at much faster rates than long cracks (for a review see (1)). The present author is, however, not aware of any short crack data generated under high temperature conditions.

The present paper provides the reader with some data on crack initiation and on microcrack growth in PM Astroloy, a candidate aero gas turbine disk material. These data are selected examples from a wider investigation, the results of which will be published elsewhere (2).

* JOINT RESEARCH CENTRE, CEC
PETTEN ESTABLISHMENT
PETTEN, P.O.B. 2, THE NETHERLANDS

Previous work by the same author (3,4) covered the identification of the time dependent processes affecting the high-temperature low cycle fatigue life over a wide range of test temperatures, strain-rates and plastic strain-amplitudes, the determination of the limits of operation of these time dependent processes and the assessment of their relative importance.

EXPERIMENTAL PROCEDURE

Material

PM Astroloy was supplied by Creusot-Loire in the form of hot isostatic pressed cylinders made of Argon atomised powder of composition (in weight %):

Cr	Co	Mo	Al	Ti	C	B	Ni
14.92	16.62	4.95	3.70	3.54	0.024	0.023	bal.

The material was HIP'ed below the γ' solvus temperature at 1403 K for six hours at 1000 bar, resulting in a grain size of 10-20 μm. Specimen blanks were trepanned from the cylinders by spark erosion and given a three step heat treatment:

4 h/1383 K/O.Q. - 24 h/923 K/A.C. - 8 h/1033 K/A.C.

The matrix is hardened by two families of γ' precipitates with dimensions of 100-200 nm and of 50-60 nm respectively. Some large γ' precipitates with dimensions of 1-4 μm remain in the matrix from the precompaction phase. Similar large γ' particles are present on the grain boundaries, blocking grain growth. The total fraction is 48 vol.%. Notwithstanding the ageing heat treatment the grain boundaries are nearly devoid of $M_{23}C_6$ carbides. The serrated form of the grain boundaries provides their strength. The carbides are primarily present in the form of TiC and are located throughout the matrix on nearly spherical surfaces which coincide with the prior powder particle boundaries.

Testing Techniques

Fatigue tests are performed on a closed loop servohydraulic testing machine with 100 KN load capacity. The test specimen has a smooth, cylindrical gauge section with a diameter of 7 mm. Strains are measured axially by means of a high temperature extensometer equipped with quartz legs which are pressed on the cylindrical gauge section. The specimen is heated by means of high frequency induction. Special care is given to specimen alignment since sample bending and buckling are known to increase scatter in LCF testing (5). Bending strains are kept below 3 percent of the average axial strains as measured at 1/10 of the maximum specimen load. All tests are performed in strain-rate control. The specimens are cycled between plastic strain limits with an R ratio equal to -1. Tests are invariably started in compression. Strain-rates in tension and in compression are equal. Temperature, load, total and plastic strain signals are continuously recorded as a function of time.

The number of cycles to crack initiation and the crack growth characteristics are determined by means of a replica technique. The LCF test is interrupted at zero load, the control mode is changed to load control and the sample allowed to cool under zero load. The entire

specimen gauge length is subsequently replicated in situ and, following reheating and changing back to strain control, the test is continued. Frequent test interruptions provide a series of replicas from which the number of cycles to crack initiation and the crack length increments are determined. The samples are electrolytically polished and etched in aqua regia to reveal the microstructure and to improve the resolution of crack initiation. Neither the electropolishing nor the frequent cooling and heating cycles applied in the replication tests appear to have an adverse effect from the point of view of LCF life when comparing the results to those obtained on mechanically polished specimens with groove depths of the order of 1 μm.

In a previous paper (3) endurance test results were reported for the following test parameter ranges:

$$673\ K \leq T \leq 1003\ K$$

$$2.10^{-6}s^{-1} \leq \dot{\varepsilon}_t \leq 1.10^{-2}s^{-1}$$

$$4.10^{-4} \leq \Delta\varepsilon_p/2 \leq 6.10^{-3}$$

Crack initiation and crack growth tests were performed under test conditions selected from the aforementioned ranges.

RESULTS AND DISCUSSION

Endurance

The endurance of PM Astroloy over the temperature range 673 K $\leq$ T $\leq$ 1003 K is a complex function of the plastic strain-amplitude (3). This is illustrated in fig. 1 for a single plastic strain-amplitude, $\Delta\varepsilon_p/2$, below the cyclic yield. With decreasing strain-rate, $\dot{\varepsilon}_t$, the number of cycles to failure, N_F, steadily decreases, showing a tendency for saturation at the lower strain- rates. The decrease in N_F with decreasing $\dot{\varepsilon}_t$ depends on the temperature and on the plastic strain-amplitude. The analysis of endurance data and of the cyclic hardening/softening behaviour in air and in vacuum, together with a study of the evolution of the precipitation microstructure and of deformation mechanisms and the corresponding dislocation microstructures, revealed the operation of four time dependent processes within the boundaries of the T - $\dot{\varepsilon}_t$ - $\Delta\varepsilon_p/2$ régime under investigation. These processes, and the limits within which they operate, are identified in fig. 2 in a T - $\dot{\varepsilon}_t$ map.

Time dependent deformation and $Cr_{23}C_6$ precipitation reactions operate over a limited range in the high temperature low strain-rate corner of the T - $\dot{\varepsilon}_t$ map. Time dependent strain accumulation, resulting from dislocation climb and accompanied by slip homogeneisation, cause a reduction in the cyclic life which is, at 1003 K, fairly limited. The unexpected increase in the endurance with decreasing strain-rate below $\dot{\varepsilon}_t = 5.10^{-5}s^{-1}$ at 1003 K in fig. 1, correlates with the precipitation of $Cr_{23}C_6$ carbides on the grain boundaries. It is conceivable that this increase in N_F is linked to a reduced susceptibility of the grain boundaries to oxygen diffusion as the result of the presence of $Cr_{23}C_6$ precipitates.

The T - $\dot{\varepsilon}_t$ conditions up to which dynamic strain-ageing (D.S.A.) is effective, fig. 2, depend on $\Delta\varepsilon_p/2$, extending to higher temperatures and smaller strain-rates for smaller plastic strain-amplitudes. The operation

of D.S.A. processes is evidenced by the occurrence of negative strain-rate sensitivity effects over specific temperature and strain-rate ranges. D.S.A. has a positive effect on endurance. The occurrence of D.S.A. is however not a sufficient condition for an effective increase in life. The beneficial effect of D.S.A. on the cyclic life may well be offset by the detrimental effect of oxidation, such as for instance under the long life conditions prevailing at small strain-amplitudes.

Oxidation effectively reduces the cyclic life of PM Astroloy under all the test conditions investigated, similar to the operation of time dependent deformation at temperatures near to and beyond approximately 1000 K. At this temperature the "mechanical" component (estimated on the basis of vacuum data), and the "oxidation" component (estimated by comparing air to vacuum data), contribute equally to the life reduction at high $\Delta\varepsilon_p/2$. At small $\Delta\varepsilon_p/2$ the "oxidation" component has an overriding effect on life.

Crack Initiation

Crack initiation is defined here as the number of cycles to initiate cracks with a length, measured on the sample surface, of approximately two grain diameters. This corresponds to crack depths of the order of one grain diameter (20 μm), as was verified on the fracture surfaces of several samples which were broken at initiation and at failure following heat tinting of the cracked surface.

Cracks invariably initiate at the specimen surface and are distributed homogeneously over the sample gauge length. In air the crack density increases with increasing plastic strain-amplitudes. The environment appears to bear a large effect on the crack density and on the number of cycles for initiation. The vacuum tests at 1003 K indeed reveal that over the entire sample gauge length only one or two cracks initiate and grow. In air, the crack density reaches values of the order of 5-15 cracks/mm (counted on a linear intercept basis along a line parallel to the stress axis) in failed specimens. At constant plastic strain-amplitude the number of cycles for initiation is smaller in air than in vacuum. At T = 1003 K, $\dot{\varepsilon}_t = 5.10^{-5}\,s^{-1}$ and $\Delta\varepsilon_p/2 = 6.10^{-4}$ for example, 25 cycles and over 2000 cycles were required to initiate a crack in air and in vacuum, respectively. Also the cracking mode is strongly environment dependent. In air, crack initiation is transgranular at 673 K, predominantly intergranular at 923 K and fully intergranular for all the strain-rates investigated at 1003 K. In vacuum, crack-initiation is transgranular up to 1003 K down to the lowest strain-rate investigated, i.e. $\dot{\varepsilon}_t = 5.10^{-5}\,s^{-1}$.

The number of cycles for crack initiation, N_I, decreases with increasing $\Delta\varepsilon_p/2$, with decreasing $\dot{\varepsilon}_t$ and partly also with increasing temperature. The life fraction for crack initiation, N_I/N_F, varies non-systematically with T, $\dot{\varepsilon}_t$ and $\Delta\varepsilon_p/2$ between 0.3 and 0.7 over the range of test conditions investigated (4). This non-systematic dependence is the result of the simultaneous operation of some of the time dependent processes indicated in fig. 2. The effect of these processes on crack initiation can be rather distinct as illustrated in fig. 3. The continuous decrease of N_I with increasing temperature at $\dot{\varepsilon}_t = 5.10^{-5}\,s^{-1}$ is the result of a dominating role of oxidation. At $\dot{\varepsilon}_t = 1.10^{-2}\,s^{-1}$ oxidation is overtaken by dynamic strain-ageing which causes a peak in N_I at approximately 900 K. The positive effect of D.S.A. on N_I can be rationalised in terms of slip dispersal. PM Astroloy deforms by a planar slip mechanism at high strain-rates up to temperatures of 1000 K. The

increase in cyclic stress which is required to deform a sample to similar plastic strain amplitudes in the D.S.A. regime as compared to the regime where D.S.A. does not operate, results in the activation of an increased number of slip bands, and hence, in a more evenly distributed slip. The number of cycles necessary to build up the critical strain for cracking within a slip band, i.e. N_I, will therefore increase.

Crack Growth

Once initiated, microcracks grow individually as well as through a process of coalescence. At 673 K crack growth is fully transgranular. At temperatures of 923 K and higher in air, the mode of crack growth changes from inter- to transgranular at crack depths which are determined primarily by the applied test temperature/strain-rate combination, the transition depth being larger the higher the temperature and the lower the strain-rate. The intergranular cracking mode is primarily the result of oxidation processes. This can be concluded from endurance vacuum tests at 1003 K which showed transgranular cracking down to the lowest strain-rate investigated, $\dot{\varepsilon}_t = 5.10^{-5}\,s^{-1}$. At this strain-rate the crack growth path follows the surfaces of the prior powder particles which are decorated with MC type carbides, as opposed to the genuine transgranular fracture path observed at $\dot{\varepsilon}_t = 1.10^{-2}\,s^{-1}$.

For life prediction purposes in "defect tolerant" based designs it is of interest to be able to predict crack growth rates. Tomkins' proposed a model which proved successful in predicting the life spent in cyclic crack growth in the high-strain regime of several high and low strength materials, both at room and at elevated temperature (6). An upper bound for the crack growth rate is given by

$$da/dN = \delta/2 \qquad (1)$$

where δ is the crack tip opening displacement. In an elastic-power law hardening material

$$\delta/2 = B.a. = a \ln \sec\left(\frac{\pi}{2}\frac{\sigma_t}{S}\right) \cdot \left[\frac{2S}{\pi E} + \frac{2\Delta\varepsilon_p}{1+n}\right] \qquad (2)$$

for small cyclic stress-strain hardening exponents n and for $\sigma_t/S > 0.5$. S is the cyclic UTS, σ_t is the maximum tensile stress in the cycle. The number of cycles to grow a crack in the elastic-plastic stress-strain field from an initial crack depth a_I to a final crack depth a_F is obtained by integration and is given by

$$N_P = 2 \ln (a_F/a_I)/B \qquad (3)$$

The factor 2 is a geometry factor which accounts for a semi-circular crack front (constrained crack). Using the appropriate values for n(3) and for σ_t, and taking the average of the yield stress and the UTS for S, the calculations yield results illustrated by the example in fig. 4. In this figure $(N_I + N_G) = N_F$ is compared with $(N_I + N_{PG}) = N_P$, where N_{PG} is the number of cycles spent in crack growth according to Tomkins' model and N_G is the experimentally observed number of cycles spent in crack growth. The prediction fits the experimental data at the lower end of the plastic strain-amplitude for $\dot{\varepsilon}_t = 1.10^{-2}\,s^{-1}$, but largely overestimates the crack

growth life at higher $\Delta\varepsilon_p/2$ and, even more so, at the lower $\dot{\varepsilon}_t$. The general trend is that model and experiment at small $\Delta\varepsilon_p/2$ match better, the lower the test temperature, and that the deviations between model and experiment at high $\Delta\varepsilon_p/2$ increase with increasing temperature. The prediction is rather insensitive to the choice of S.

In phenomenological terms the reasons for the lack of correlation between experimental data and the predictions based on Tomkins' model follow from fig. 5. The plot shows the observed crack growth rates as a function of crack depth for two test conditions (solid lines) at 673 K and at 923 K, for which the model prediction fits, respectively overestimates, the lives spent in crack growth. The dashed lines represent the crack depth dependence of the crack growth rates as predicted by Tomkins' model for the same test conditions. It is obvious that the good match between model and experimental data under particular test conditions, as shown in their integrated form in fig. 4 for the high $\dot{\varepsilon}_t$ and small $\Delta\varepsilon_p$, is a coincidence rather than the result of a correct prediction of the crack growth characteristics of the material.

Up to crack depths of approximately 10 times the grain size the crack growth rate is constant, displaying "short crack behaviour". Beyond that crack size the growth rates increase according to a law of the form

$$da/dN = C.a^q.f(\Delta\varepsilon_p/2), \tag{4}$$

the exponent $q \simeq 2$ and C being a constant. Tomkins' model, on the other hand, predicts a linear dependence on crack depth:

$$da/dN = B.a \tag{5}$$

It is conceivable that the high growth rates observed for cracks with depths beyond the short crack regime are caused by environmental effects and by crack coalescence, which is observed experimentally to contribute to the crack growth process.

In fig. 6 the crack growth rates at T = 923 K, $\dot{\varepsilon}_t = 1.10^{-2}s^{-1}$, $\Delta\varepsilon_p/2 = 1{,}5.10^{-3}$ are compared with long crack growth data from the literature in terms of ΔK. Both Pelloux and Huang's (7) and Gayda and Miner's (8) data hold for material with nearly similar grain sizes as the PM Astroloy used in the present investigation, although the precipitation microstructure differs in terms of volume fractions of precipitates and precipitate morphology. Another difference resides in the different R values being applied. Despite these differences all the data, including data from the present investigation beyond crack depths of approximately 0.25 mm (corresponding to $\Delta K \simeq 30$ MPa $\sqrt{m}$), are within a fairly narrow band. For a given ΔK the highest crack growth rate is, at maximum, a factor of 3 times the smallest rate. Below crack depths of 0.25 mm the present short crack data show growth rates far in excess of the long crack data reported in the literature. Ritchie and Suresh (1), in their review of short crack behaviour, quote the inappropriate use of linear elastic analysis as one possible explanation for the occurrence of the high growth rates of short cracks. A reanalysis of the present crack growth data in terms of ΔJ is shown in fig. 6. Based on Shih and Hutchinson's (9) work for elastic-plastic crack growth the following expression for ΔJ was adopted for the cyclic loading case:

$$\begin{aligned}\Delta J &= \Delta J_e + \Delta J_p \\ &= \xi \Delta W_e . a . \frac{1}{(1-a/b)} . f\left(a/b, 1\right) \\ &\quad + \Delta W_p . \left(\frac{n+1}{n}\right) . a . \frac{1}{(1-a/b)^n} . f\left(a/b, n\right)\end{aligned} \tag{6}$$

ΔW_e and ΔW_p are the elastic and plastic components of the remote strain energy density, a/b is the crack depth/specimen diameter ratio. Following Dowling (10) a combined surface and flaw shape correction factor of 0.51 is applied to ΔJ in order to account for the crack geometry. It is obvious from fig. 6 that the high growth rates for short cracks persist even when analysed in terms of ΔJ. There are some indications which suggest that environmental effects can be excluded as a cause for the high growth rates observed, leaving reduced crack closure (1) as a possible explanation. These indications relate to similarity of the oxidation reaction products at the tips of both long and short cracks, suggesting similar environments, and to the insensitivity to the test temperature of short-to-long crack transitions in terms of crack depth. Further tests are planned to investigate this.

SUMMARY

Under high-temperature low cycle fatigue conditions the endurance, the number of cycles to crack initiation and, consequently, also the crack growth rate of PM Astroloy depend in a complex way on the testing parameters T, $\dot{\varepsilon}_t$ and $\Delta\varepsilon_p/2$. This results from the operation, individually or simultaneously, of several time dependent processes like oxidation and dynamic strain-ageing which have a negative and a positive effect, respectively, on the fatigue properties. Crack growth data, obtained by replicating the surface of smooth test samples, correlate well with long crack growth data reported in the literature for crack depths exceeding 0.25 mm. Smaller cracks display growth rates far in excess of the growth rates of long crack data.

SYMBOLS

a, a_I, a_F = crack depth, initial and final (m).

a/b = crack depth/specimen diameter.

da/dN = crack growth rate (m/cycle).

E = Young's modulus (MPa).

ΔJ = cyclic J-integral (MPA.m).

ΔK = stress intensity range (MPa.$\sqrt{m}$).

n = cyclic stress-strain exponent.

N_I, N_F, N_G, N_p = number of cycles to crack initiation; to failure; spent in crack growth; predicted (cycles).

R = ratio of minimum to maximum plastic strain.

S = cyclic ultimate tensile strength (MPa).

T = temperature (K).

ΔW = strain energy density.

$\dot{\varepsilon}_t$ = total strain-rate (s^{-1}).

$\Delta\varepsilon_p/2$ = plastic strain amplitude.

δ = crack tip opening displacement.

σ_t = maximum tensile stress in a cycle.

ν = test frequency (Hz).

D.S.A. = dynamic strain ageing.

C.I. = crack initiation.

REFERENCES

1. Ritchie, R.O., and Suresh, S., "Behaviour of short cracks in airframe components" AGARD Conference Proceedings, no. 328, (1983) 1-1.

2. Bressers,J., to be published.

3. Bressers, J., Roth, M., Tambuyser, P., and Fenske, E., "The effect of time dependent processes on the LCF life of gas turbine disk alloys", Final report COST 50/II, report EUR 8162, (1983).

4. Bressers, J., and Roth, M., "ASME International Conference on Advances in Life Prediction Methods", eds. Woodford, D.A., and Whitehead, J.R., Book no. H00255, ASME, (1983) 85.

5. Bressers, J., "Load Axiality in Mechanical Testing", Measurement of High-Temperature Mechanical Properties of Materials, eds. Loveday, M.S., Day, M.F., Dyson, B.F., HMSO London, (1982) 278.

6. Tomkins, B., Sumner, G., and Wareing, J., "Proceedings of the International Symposium on Low Cycle Fatigue Strength and Elasto-Plastic Behaviour of Materials", Deutscher Verband für Materialprüfung e.v., Berlin, (1979) 495.

7. Pelloux, M.P., and Huang, J.S., "Creep-Fatigue-Environment Interactions", eds. Pelloux, M., and Stoloff, N.S., The Metallurgical Society of AIME, (1980) 151.

8. Gayda, J., and Miner, R.V., Metallurgical Transactions A, 14A, (1983) 2301.

9. Shih, C.F., and Hutchinson, J.W., Journal of Engineering Materials and Technology, 98, (1976) 289.

10. Dowling, N.E., "Cycling Stress-Strain and Plastic Deformation Aspects of Fatigue Crack Growth", ASTM STP 637, (1977) 97.

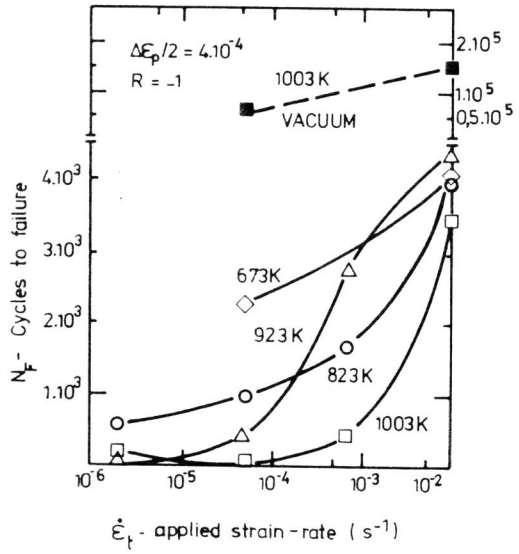

Fig. 1 - Dependence of the endurance, N_F, of PM Astroloy on the strain rate at a fixed plastic strain amplitude below cyclic yield. The plot shows the effects of the test temperature, and, at 1003 K, also of the environment.

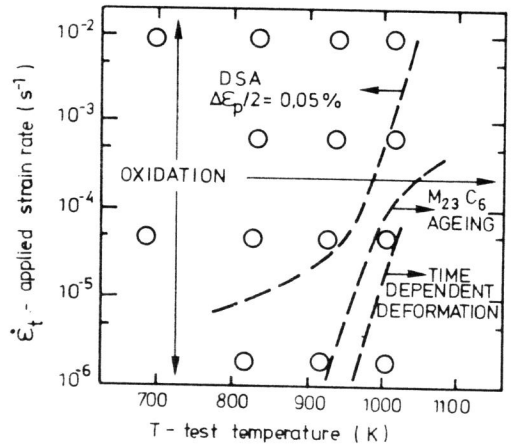

Fig. 2 - Map identifying the time dependent processes which influence the cyclic life of PM Astroloy.

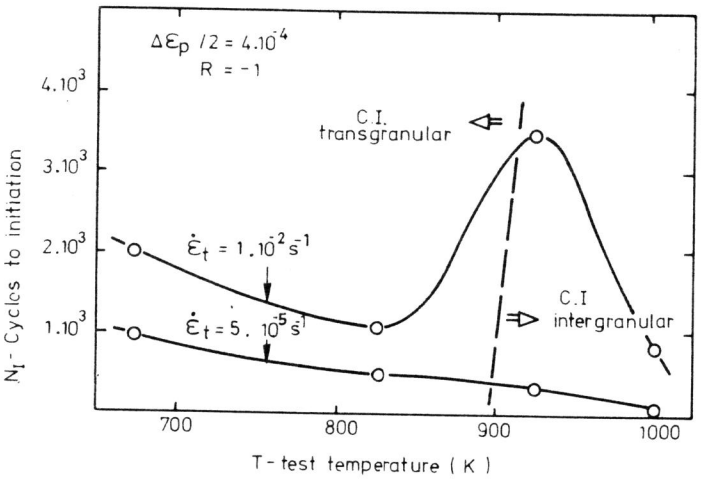

Fig. 3 - Number of cycles to initiate a microcrack in PM Astroloy in air as a function of the test temperature for two different strain-rates.

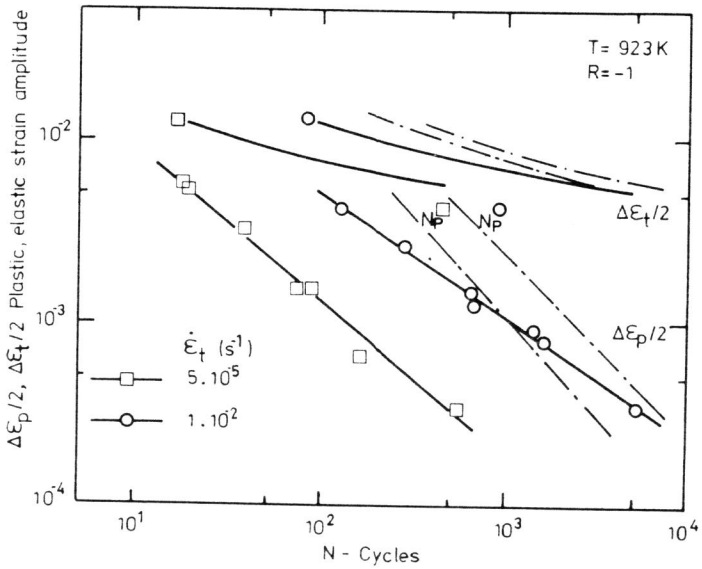

Fig. 4 - Comparison between the predicted (N_p) and observed number of cycles to failure in air (full lines) in PM Astroloy for two strain-rates.

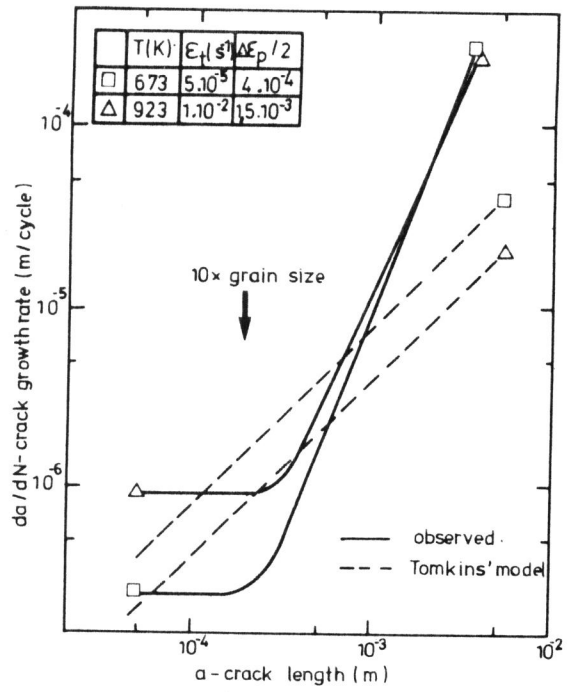

Fig. 5 - Observed and predicted crack growth rates in air as a function of the crack depth a.

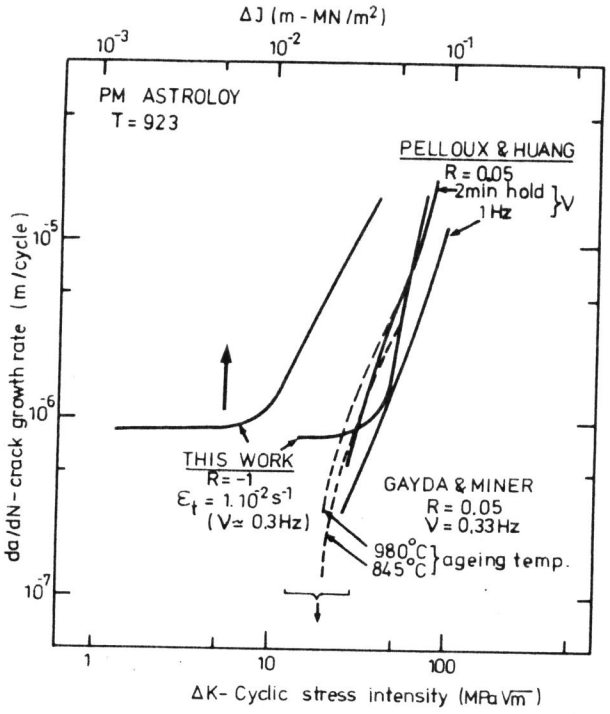

Fig. 6 - Crack growth rates at 923 K as a function of ΔK (bottom) and comparison with literature data and as a function of ΔJ (top).